A novel multilayer immunoisolating encapsulation system overcoming protrusion of cells

Bhujbal, Swapnil V.; de Haan, Bart; Niclou, Simone P.; de Vos, Paulus

Link to publication in University of Groningen/UMCG research database

OPEN

A novel multilayer immunoisolating encapsulation system overcoming protrusion of cells

Swapnil V. Bhujbal[1,2], Bart de Haan[1], Simone P. Niclou[2] & Paul de Vos[1]

[1]Department of Pathology and Medical Biology; Immunoendocrinology, University of Groningen, Hanzeplein 1, 9700 RB Groningen, The Netherlands, [2]NorLux Neuro-Oncology Laboratory, Department of Oncology, Centre de Recherche Public de la Santé, Luxembourg.

Application of alginate-microencapsulated therapeutic cells is a promising approach for diseases that require a local and constant supply of therapeutic molecules. However most conventional alginate microencapsulation systems are associated with low mechanical stability and protrusion of cells which is associated with higher surface roughness and limits their clinical application. Here we have developed a novel multilayer encapsulation system that prevents cells from protruding from capsules. The system was tested using a therapeutic protein with anti-tumor activity overexpressed in mammalian cells. The cell containing core of the multilayer capsule was formed by flexible alginate, creating a cell sustaining environment. Surrounded by a poly-L-lysine layer the flexible core was enveloped in a high-G alginate matrix that is less flexible and has higher mechanical stability, which does not support cell survival. The cells in the core of the multilayer capsule did not show growth impairment and protein production was normal for periods up to 70 days *in vitro*. The additional alginate layer also lowered the surface roughness compared to conventional cell containing alginate-PLL capsules. Our system provides a solution for two important, often overlooked phenomena in cell encapsulation: preventing cell protrusion and improving surface roughness.

Immunoisolation of cells for implantation purposes is based on enveloping the cells in a biocompatible and semipermeable membrane that allows diffusion of essential nutrients and therapeutic molecules but prevents deleterious effects of the humoral and cellular part of the host immune system[1,2]. The technique is proposed for the delivery of cell based therapeutics where local and minute-to-minute release of the active molecule is desired for effective treatment. Encapsulation of living cells for the release of biological therapeutics is under investigation for a variety of diseases such as diabetes[3], neurological diseases[4–7], and cancer[8–10].

A commonly applied technology of immunoisolation is microencapsulation of therapeutic cells in spherical beads made of alginate polymers[11] using different encapsulation techniques like electrostatic bead generator, jet cutter, vibrating nozzle, and coaxial air driven droplet generator[12]. Spherical beads are often preferred over discs or tube like structure because of the favorable surface-to-volume ratio which facilitates nutrition of the cells and the release of therapeutic agents[11]. Another argument to favor microcapsules is the relative small size that allows for transplantation in many sites without interference with the receiving organ[11]. The latter is an important consideration for example in the treatment of brain tumors, where implantation of microencapsulated cells producing anti-tumor agents has been proposed as an effective approach to delete remnants of malignant cells[13,14]. Invasive brain tumor cells are impossible to recognize and eliminate during surgery and are a major cause of morbidity.

Microcapsules that are being proposed for diseases such as for the treatment of brain tumors should meet a number of requirements. A key feature in designing immunoisolating microcapsules is avoiding protrusion of cells from capsules. Most conventional alginate encapsulation systems do not meet this prerequisite, as protrusion of cells is more the rule than an exception (figure 1). Protrusion of cells is associated with rejection and fibrotic responses followed by necrosis of the therapeutic cells, which ultimately leads to graft failure[15]. Another danger is that the therapeutic cells based on cell lines may form tumors themselves when they leak out of the capsules. This is a major safety hurdle preventing the application of cell encapsulation technology in the clinic. Therefore cell based therapy requires a system in which protrusion of cells is prevented.
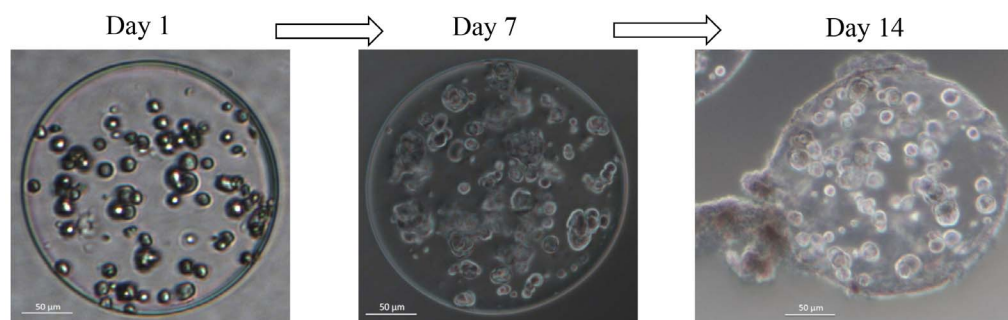
Figure 1 | **Cell growth leads to protrusion of cells over time.** Protrusion of cells always occurs in conventional alginate-encapsulation systems.

Alginate is the most commonly applied polymer for cell encapsulation, due to its biocompatibility, ease of processing and heat stable nature[16,17]. Alginate is a polysaccharide of linear copolymers of (1–4) glycosidically linked α L-guluronic acid (G) and its C-5 epimere, β D-mannuronic acid (M) residues. The relative amount of the two uronic acid monomers as well as their sequential arrangement along the polymer chain differs widely. The uronic acid residues are distributed along the polymer chain in a pattern of binary blocks: G-G blocks, M-M block, or M-G blocks. Based on the composition of G and M residue, alginate is classified as high-G alginate (G content ≥ 60%), intermediate-G alginate (G content in range of 40–60%), and low-G alginate (G content ≤ 40%). The composition as well as the molecular weight of alginate determines the physiochemical properties of the capsules, which also affect cell function[18]. The aim of the present study was to develop a novel multilayer capsule which overcomes protrusion of cells and high surface roughness while maintaining efficacy of secretion of the therapeutic protein. In the novel system we applied alginate with different mechanical stabilities to facilitate growth of the cells in the core of the capsules but to kill cells that might escape from the capsule and invade the host (figure 2a).

Results

To prevent cell protrusion from alginate capsules, we applied different types of alginate to produce gels with different mechanical stability[19]. The 3.4% intermediate-G alginate beads gelled in 100 mM $CaCl_2$ solution had a rigidity of 9.47 ± 1.61 g and an elasticity of 7.99 ± 0.76 s. The 2% high-G alginate beads were more rigid (11.05 ± 0.77 g) and less elastic (9.12 ± 0.57 s) than 3.4% intermediate-G alginate beads. A too rigid environment will lead to deregulation of cellular metabolism and protein synthesis, eventually leading to cell death. The tests were performed with a mammalian cell lines (BHK cells), as these cells are often applied in preclinical models for the release of therapeutic agents[9,20]. BHK cells were encapsulated in alginates with two different rigidities and elasticities after which functional survival was studied. The methodology to make multilayer capsules is described in the method section (figure 2b).

Long-term survival and protection of outgrowth of BHK cells in different alginate types. We then investigated the survival of the cells at different periods of time in 3.4% intermediate-G alginate capsules and 2% high-G alginate beads. Cell survival was monitored on a weekly basis and images were acquired on day 1, 7, 14, 21, and day 28 as shown in figure 3. Within 1st week, BHK cells encapsulated in 3.4% intermediate-G alginate started to grow without obstruction and formed cellular clusters. By day 28, these capsules were completely filled with cells. This was very different in the more rigid 2% high-G alginate capsules. Cell growth was impaired when compared to the cells in the 3.4% intermediate-G alginate. On day 28 most of the cells encapsulated in 2% high-G alginate were dark and necrotic indicating that 2% high-G alginate hampers cell survival.

Cell behavior in the multilayer system. To determine whether the multilayer system caused an impairment in cell survival, we studied the viability of BHK cells in the multilayer system in comparison to the conventional 3.4% intermediate-G alginate APA capsules. Viability studies were done on at day 1, 7, 14, 21, 28, 35, 49, 56, 63, and day 70. As shown in figure 4a cell survival and growth in both the control 3.4% intermediate-G alginate APA capsules and in the multilayer capsules steadily increased from day 1 to day 70. Cells in the multilayer capsules grew slower. The multilayer capsules were completely filled by day 49, whereas the 3.4% intermediate-G alginate APA capsules were already filled by day 28. Live dead quantification of cells shows approximately 85% of live cells in both conventional and multilayer capsules at any given time point.

Outgrowth of cells in the control capsules was observed by day 14. This was associated with cell growth in the culture flask. In the multilayer capsule cultures we did not observe cells in the flask. Cells in multilayer capsules started to migrate to the outer layer as of day 28, but were trapped effectively and died (figure 4b). To summarize we show that multilayer capsules prevent protrusion of cells *in vitro*.

Multilayer capsules secrete therapeutic proteins for prolong periods of time. We quantified the secretion of therapeutic sLrig1 from 50 multilayer capsules, cultured in 96 well plates with 100 μl of culture medium. The culture supernatant was collected and replaced with fresh culture medium twice a week from day 14 till day 70. The secretion of sLrig1 was detected by Western blot and quantified as percentage of secretion of sLrig1 with respect to day 14 (figure 4c). The secretion of sLrig1 increased exponentially till day 42, where the highest secretion was observed. After day 42 the secretion was relatively stable with slight fluctuations in secretion of sLrig1 until day 70. As mentioned above traditional 3.4% intermediate-G alginate APA capsules showed protrusion and growth of cells in the culture flask, therefore the secretion of sLrig1 from the APA capsules cannot be reliably quantified. Therefore we restricted quantification of sLrig1 from multilayer capsules.

Cell load and cell growth increases surface roughness of capsules. Surface roughness of the capsules as a consequence of cell growth is correlated with host responses[21]. We therefore questioned how protrusion of cells influences surface roughness. To this end we studied surface roughness of cell containing APA capsules and multilayer capsules; APA capsules without cells were used as control. Analysis was done on day 30 post encapsulation. As shown in figure 5, APA capsules with cells (Rq=20.84 ± 15.13) had a significant higher surface roughness compared to empty APA capsules (Rq=1.65 ± 0.35) (p <0.05). Although there was a tendency that surface roughness of multilayer capsules with cells (Rq=11.53 ± 2.82) had lower surface roughness compared to APA capsules with cells, the difference was not statistically significant. There was also no significant difference between surface roughness of empty APA capsules and cell containing
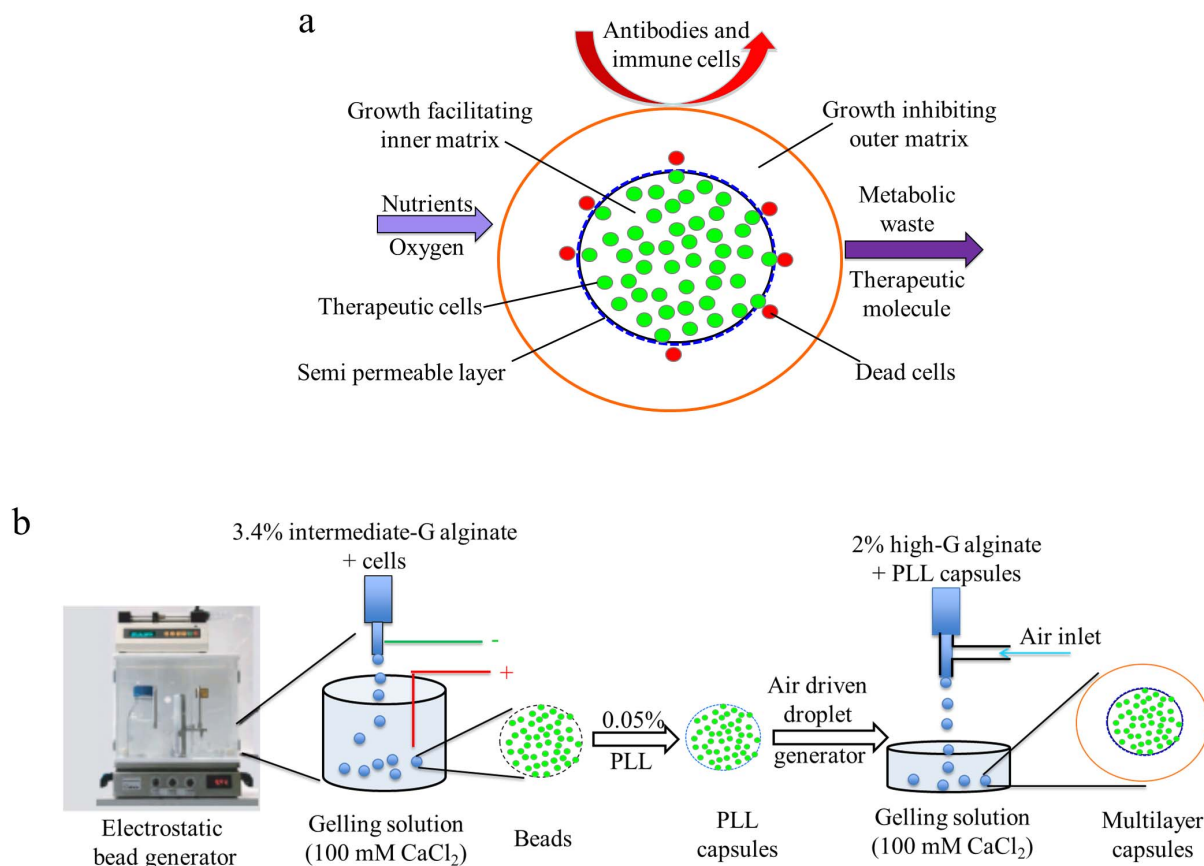
Figure 2 | (a) Schematic representation of the novel multilayer capsule concept avoiding protrusion of cells. The core of multilayer capsules facilitates growth of cells while the outer shell of the capsule traps escaping cells and induces cell death. (b) Schematic representation of methodology to generate multilayer capsules. Briefly after coating alginate-PLL capsules, the alginate-PLL capsules are reencapsulated with growth inhibiting 2% high-G alginate matrix. (Details in materials and methods).

multilayer capsules. In conclusion we find that cell growth and protrusion increase the surface roughness of capsules, and this may be ameliorated in multilayer capsules.

Discussion

The fact that mechanical strength of alginate influences cell behavior is based on the principle of mechanotransduction. Mechanotransduction is a process by which mechanical forces acting on cells influence biochemical cell behaviour and viability[22–24]. This principle of mechanotransduction was applied to design a multilayer capsule with a minimal risk of protrusion of therapeutic cells. The system does not involve the inclusion of toxic components or any other molecules that might interfere with the survival of the encapsulated cell or with the host tissue. It is simply based on applying a rigidity on the outside of the capsule that is not compatible with cell survival. To our best knowledge we are the first to demonstrate this principle in microencapsulation systems. Different cells require different circumstances for optimal survival[18,25]. For every cell type it may be necessary to adapt the alginate with cell facilitating and inhibitory properties. Here we used calcium-alginate because the rigidity to kill BHK cells was already reached with this alginate-divalent cation combination. We have also tested the efficacy of multilayer capsules in preventing protrusion of human embryonic kidney cells (supplementary figure 1).The rigidity however can be further enhanced by applying divalent cations with a higher affinity for alginates (Pb>Cu> Cd> Ba> Sr> Ca> Co> Ni> Zn> Mn> Mg)[26]. Thus by using divalent cations with a higher affinity for alginate such as Pb^{2+}, Cu^{2+}, Cd^{2+}, or Ba^{2+} the rigidity can be gradually increased[27,28]. Notably, application of Pb^{2+}, Cu^{2+}, and Cd^{2+} must be

avoided because they are toxic to cells. Another effective method for increasing alginate rigidity is increasing the G-content or increasing the concentration of the alginate to create a mechanotransduction environment not compatible with cell survival. The molecular processes and sensors by which mechanotransduction occurs is still largely unknown[23,29]. Recent studies have suggested that integrin's play a key role in mechanotransduction[30,31]. Since alginate lacks integrin binding sites[32], non-integrin dependent mechanotransduction may occur which must be responsible for the observed effects on cell behavior[33].

Similarly different cells may require different conditions for optimal survival in the capsule core[18,25]. The advantage of the multilayer system is that the inner capsule is not in direct contact with the microenvironment in the host. This implies that within the multilayer system the balance between optimal biocompatibility in the host and optimal cell-survival environment is less strict[34–38]. The multilayer system also may improve the surface roughness as shown in figure 5. Another issue that is overcome by the novel system is the reported variations in PLL binding and the associated host responses[21,39–41]. PLL is often applied to the alginate beads in order to reduce the pore size. Immunoprotective systems should protect the encapsulated cells against high molecular weight effector molecules of the adaptive immune system such as immunoglobulins and complement factors[2]. The PLL capsules usually have a permeability that allows for diffusion of molecules below 160 kDa[2,42]. However binding of poly-aminoacids to alginate beads is not straightforward. Alginate should form a superhelical core around the PLL and the PLL itself should be forced into β-sheets[40]. This requires an ion exchange process which if not correctly done leads to host responses against

	3.4% intermediate-G alginate APA capsule	2% high-G alginate beads
Day 1		
Day 7		
Day 14		
Day 21		
Day 28		
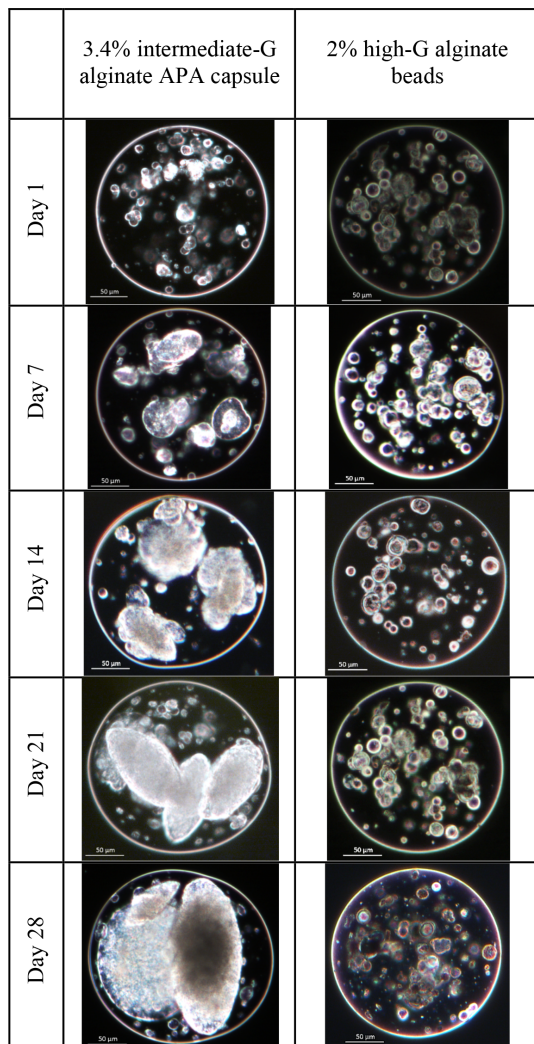
Figure 3 | Mechanical stability of alginate influences cell growth. Phase contrast microscopic images of BHK-cell growth in 3.4% intermediate-G alginate-poly-L-lysine (APA) capsules, and 2% high-G alginate beads. APA capsules facilitate cell growth while 2% high-G alginate inhibited cell growth.

inadequately bound PLL[39,41,43,44]. This is considered to be one of the factors contributing to the low degree of reproducibility of alginate-polyamino-acid encapsulation[38,43–45]. This binding is less important when the PLL-layer can be covered with an additional layer of alginate with a documented high degree of biocompatibility[39,40]. Therefore the multilayer capsule procedure may contribute to reproducibility. Moreover the high crosslinking of gelling ions in high-G alginate reduces the pore size of multilayer capsules.

Even though the high crosslinking network obtained with high-G alginate, results in smaller pore sizes and increases rigidity, diffusion of nutrients and secretion of 100 kDa recombinant sLrig1 from encapsulated cells was not obstructed in multilayer capsules. The observed fluctuations in secretion after day 42 can be attributed to cellular contact inhibition or deprivation of nutrients and oxygen in the core of the capsules[46]. It is difficult to assess the exact concentration of sLrig1 released from the capsules. Based on antibody staining, we can only provide a relative quantification. However the amount of sLrig1 secreted from encapsulated BHK-sLrig1 cells depends on the initial cell concentration and doubling time for cells. With the current settings, we obtained approximately 17 fold increase of sLrig1 secretion per bead on day 42 with respect to day 14. In the past we have shown 40–60% inhibition of glioma growth using 5 alginate

beads encapsulated with BHK-sLrig1 cells in mouse models[9]. It is likely that the initial cell load used for encapsulation and/or number of beads implanted can be increased to achieve higher efficacy.

It might be argued that the rigidity of 11.05 g for the 2% high-G gel is also interfering with host-compatibility or biocompatibility by forming a too stiff layer for host tissues in the vicinity of the capsules. In this study however we applied only alginate-types and concentrations that have already been tested *in vivo* in different implantation sites including the brain[47] and did not show any toxicity or severe response in the host[41,47,48]. It seems that intracapsular rigidity is a different issue than surface rigidity[49,50] which previously has been reported to be a critical issue for biocompatibility[51,52].

The surface roughness of microcapsules also plays a crucial role in host responses. A high Rq is associated with enhanced adsorption of proteins and inflammatory cells[48,51,52]. Although the Rq value of APA capsules with and without cells was not statistically significant from the multilayer capsules with cells, we postulate that providing an additional alginate layer may reduce the variations induced by cell inclusions. In the present study we show that loading the system with cells leads to increased surface roughness as cell free APA capsules had a lower surface roughness than cell containing APA capsules and multilayer capsules. This suggests that inclusion of cells affects the gellification process. Increasing the cell load, hinders the cross linking of gelling ion and as a consequence decreases mechanical stability[19]. This further increases protrusion and surface roughness. As protrusion is a random phenomenon, protrusion or disruption of the surface structure can occur anywhere on the surface and in different degrees as shown by large standard deviations values in this study. We found that APA-capsules sometimes had Rq values varying in range between 3.34 nm and 40.3 nm. Previous AFM studies have been conducted on cell free capsules which did not report large variations on APA capsules[21]. We suggest that the variation in surface in cell containing capsules observed in our study may contribute to the reported variations in host responses (biocompatibility) against APA-encapsulated cells. Cell load[13,42,53] and surface roughness are interrelated and do matter for *in vivo* success of implanted capsules[51,52]. Moreover it has been shown that the Rq of alginate beads increases with increasing affinity of the divalent cations for alginate[51,52]. By using divalent cations with a higher affinity for alginate the surface roughness of alginate capsules can be gradually increased. Therefore, to keep the surface roughness low on the multilayer system we recommend to use calcium ions as long as high-G alginate is applied.

Conclusion

A system in which protrusion of cells is prevented is mandatory for cell based therapies. In particular with encapsulated therapeutic cell lines, outgrowth of these cells from the capsules may lead to tumor formation. Here we report on a novel microencapsulation system that strongly reduces cell protrusion of cells. Different types of highly biocompatible alginates were applied to facilitate growth and survival of therapeutic cells in the core of the capsules while destroying cells escaping from the core of multilayer capsule. Studies are ongoing to determine the efficacy of this system in pre-clinical models *in vivo*.

Methods

Alginate purification. Alginates of different compositions were obtained from ISP Alginates Ltd UK. Two types of alginates have been purified: 1) intermediate-G alginate (containing 44% G-chain residues, 56% M-chain residues, 23% GG-chain residues, 21% MG-chain residues, 37% MM-chain residues) and 2) high-G alginate (containing 67% G-chain residues, 33% M-chain residues, 54% GG-chain residues, 13% MG-chain residues, 21% MM-chain residues). Alginates were purified in-house as described in detail elsewhere[54]. Briefly 12–15 gm of crude alginate was dissolved in ice cold 1 mM Na-EGTA (ethylene glycol tetraacetic acid), under constant stirring. The dissolved alginate was filtered through 5 µm, 1.2 µm, 0.8 µm, 0.45 µm filter (Whatman®, Dassel, Germany), to remove visible aggregates. Subsequently the pH of the solution was carefully lowered to 2 with 2 N HCL +20 mM NaCl on ice. Lowering of pH causes alginate to precipitate as alginic acid. Alginic acid precipitate
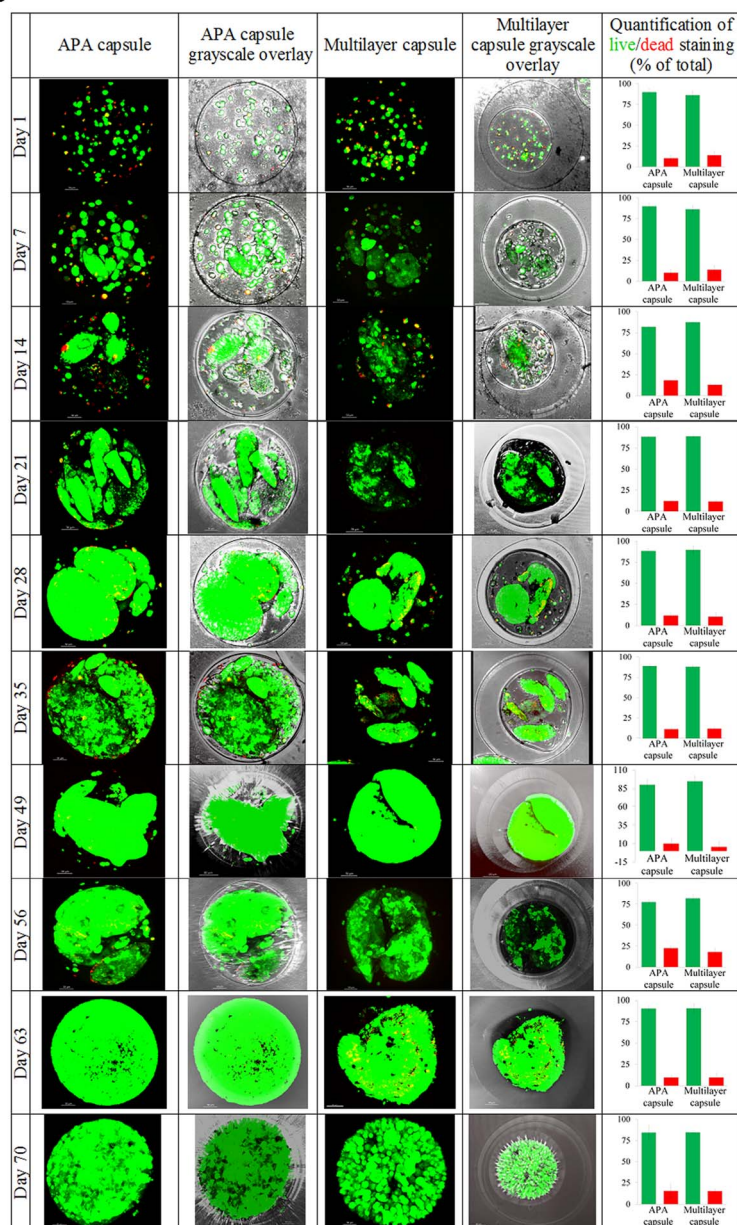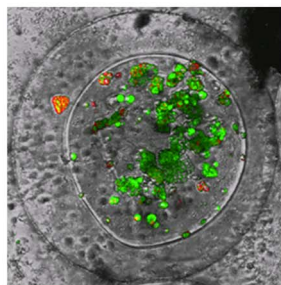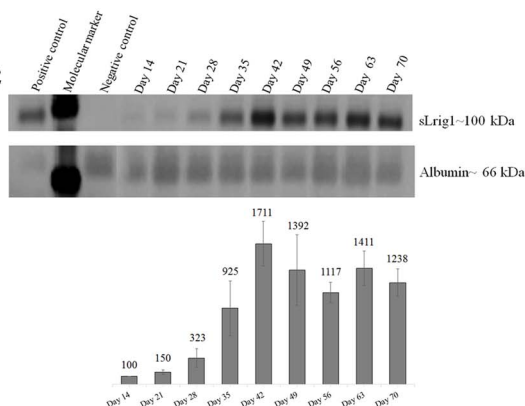
Figure 4 | Cell growth and survival in intermediate-G alginate APA capsules and in the inner core of multilayer capsules. (a) Confocal microscope images and quantification (n=3) of live- dead encapsulated BHK cells in APA capsules and multilayer capsule after live-dead staining at different time points. Live cells emit green fluorescence, dead cells emit red fluorescence. (b) Proof of concept of multilayer capsule: localization of live (green) and dead (red) BHK cells in a multilayer capsule. Protruding cells are effectively killed in multilayer capsules. (c) Western blot (n=3) analysis of secreted sLrig1 protein (upper band) from BHK-sLrig1 cells encapsulated in multilayer capsules. Multilayer capsules secrete sLrig1 for prolonged periods of time. Bovine serum albumin is visualized by nonspecific binding of secondary antibody (lower band).

Rq- 1.65 nm   Rq- 20.84 nm   Rq- 11.53 nm
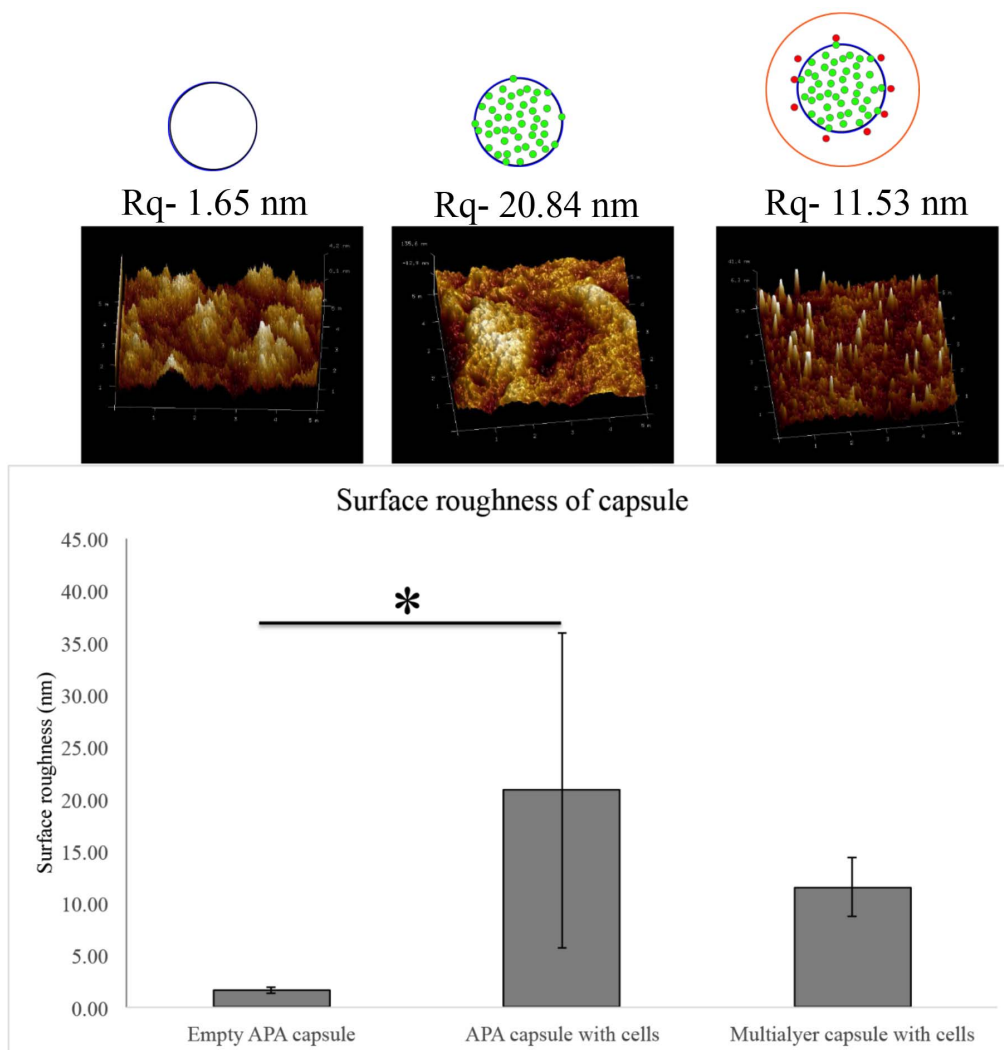
Figure 5 | Cell load, cell growth and alginate type affect surface roughness of the capsule. Surface roughness (Rq) of intermediate-G alginate-PLL-alginate (APA) capsules without cells, with cells and in multilayer capsule with cells on day 30 post encapsulation (n=4). Cell load increases the surface roughness of capsules. Multilayer capsules with cells show a tendency towards lower surface roughness than APA capsules with cells. Values are expressed as mean $\pm$ SD, *$p < 0.05$.

was filtered through a Buchner funnel of pore size 1.5 mm and washed with 1 liter of 0.01N HCL + 20 mM NaCl to remove non precipitated contaminants. Next the proteins from the aggregate alginate acid were removed by chloroform : butanol (4 : 1 ratio) extraction. The mixture was vigorously shaken for 20 minutes. The suspended mixture was filtered over Buchner funnel. Chloroform : butanol extraction step was repeated twice. Subsequently the alginic acid was then bought into water by slowly and carefully increasing the pH to 7 with 0.5 N NaOH + 20 mM NaCl over a period of at least 1 hr. The alginate solution obtained was further treated with chloroform : butanol (4 : 1 ratio) to remove proteins which can only be dissolved in at neutral pH. The mixture was centrifuged for 3 minutes at 1800 rpm, which induced the formation of separate chloroform : butanol phase, which was removed by aspiration. This step was repeated one more time. The last step of purification is precipitation of alginate from alginic acid using ethanol. To each 100 ml of alginate solution we added 200 ml absolute ethanol. Constant stirring for 10 minutes in ethanol led to precipitate alginate. The alginate was filtered over the Buchner funnel and washed two times with absolute ethanol. Later, the alginate was washed three times with diethyl ether and was freeze-dried overnight. After purification 3.4% (w/v) intermediate-G alginate and 2% (w/v) high-G alginate were dissolved at 4°C in Krebs–Ringer–Hepes (KRH) with an appropriate osmolarity and further sterilized by 0.2 μm filtration (Corning®, NY, USA).

Mechanical stability of empty beads. Empty beads of 3.4% intermediate-G alginate beads and 2% high-G alginate were made using air driven droplet generator using 23 g needle, gelled in 100 mM CaCl$_2$ for 5 minutes as previously described by us[19]. Mechanical stability of alginate capsule can be quantified using different methods like burst pressure[55], ultrasound[56], Young's modulus[57], however we prefer to calculate the mechanical stability based on force and time required to resist compression[19]. The

mechanical stability was quantified with a Texture Analyzer XT plus (Stable Micro Systems, Godalming, UK) equipped with a force transducer with a resolution of 1 mN as previously described by us[19]. Texture Exponent software version 6.0 was used for analyzing the data. Briefly individual beads of size 500 μm micrometer were carefully sorted using a dissection microscope (Leica MZ75 microsystems) equipped with an ocular micrometer with an accuracy of 25 μm. Individual beads were carefully placed on plate, storage solution was carefully removed. The mechanical stability of beads was measured by compressing individual microcapsules to 60% using P/25L mobile probe with a pretest speed of 0.5 mm/sec, a test speed of 0.01 mm/sec, and a posttest speed of 2 mm/sec. The trigger force was set to 2 grams. The force exerted by the probe to compress the bead was recorded as function of time.

Cell microencapsulation. Baby hamster kidney (BHK) cells expressing anti-tumor protein sLrig1 (soluble leucine rich repeats and immunoglobulin like domain1) a negative regulator of growth factor signaling[9] were grown in DMEM medium supplemented with 4.5 g/L glucose, 10% (v/v) fetal bovine serum (compliment deactivation), 1% (v/v) Antibiotic-Antimycotic (100X) (Sigma-Aldrich,). BHK control and BHK-sLrig1expressing cells at concentrations of 6 × 10⁶ cells per milliliter of sterile 3.4% intermediate-G alginate or 2% high-G alginate were carefully mixed and were transferred into droplets with an electrostatic bead generator, using a 27 g needle. The droplets were collected in 100 mM CaCl$_2$ as gelling solution for 5 minutes. Subsequently, intermediate-G alginate beads were incubated with sterile (0.2 μm filtered) 0.05% poly-L- lysine (PLL) (poly-L-lysine-HCl, Mw 22 kDa, Sigma-Aldrich, The Netherlands) for a period of 3 minutes on ice and 4 minutes at room temperature. PLL coated capsules were subsequently incubated with 0.34% intermediate-G alginate in calcium-free KRH solution with an osmolarity of 310 to form alginate-poly-L-lysine alginate (APA) capsule. Next the cell-containing

intermediate-G alginate-PLL membrane was suspended in a 2% high-G alginate solution. After careful mixing the solution was brought in another type of droplet-generator using a 23 g needle and 100 mM CaCl₂ as gelling solution[58,59]. This step is meant to form multilayer capsules. A schematic workflow of making the multilayer capsules is shown in figure 2b. The encapsulated cells were subsequently cultured in 25 cm² culture flasks containing 5 ml growth medium (Dulbecco's Modified Eagle's culture medium (DMEM) supplemented with 4.5 g/L glucose, 10% (v/v) fetal bovine serum (compliment deactivation), Antibiotic-Antimycotic (100X) 1% (v/v) Sigma-Aldrich,) and kept in a standard tissue culture incubator with 5% CO₂, at 37°C. Medium was changed thrice a week. The diameters of the beads and capsules were measured with a dissection microscope (Leica MZ75 microsystems) equipped with an ocular micrometer with an accuracy of 25 μm. The 2% high-G alginate beads and APA capsules had diameter of 250–350 μm while the final multilayer capsules had a diameter of 550–650 μm.

Viability and live-dead quantification of encapsulated cells. Viability of BHK-sLrig1 cells encapsulated in APA capsules and multilayer capsules was studied with a live-dead staining kit of Invitrogen (Calcein AM (4 mM), Ethidium homodimer-1 (2 mM)). Cell containing capsules were washed three times with KRH solution containing 2.5 mM CaCl₂. Capsules were incubated in the dark for 30 minutes in 2 ml of serum free medium containing 1 μl of calcein AM and 2 μl of ethidium homodimer-1. Subsequently capsules were washed five times with KRH solution containing 2.5 mM CaCl₂. Stained cells in capsules were visualized by a Leica TCS SP2 AOBS confocal microscope and objective HC PL APO CS 10x/0.30 dry, 11 mm. An Argon laser was used for excitation of calcein AM and the emission light over 505 nm and 530 nm was measured for live cells. A Helium Neon 543 nm laser was used for excitation of ethidium homodimer-1 and the emission light over 650 nm detected for dead cells. The pictures of sections were taken through entire Z-axis through the capsules. Imaris (R) x64 version 7.6.4 software was used to process the raw data to construct 3D images and quantify live-dead cells. Viability and live-dead quantification of cells in capsules was determined on day 1, 7, 14, 21, 28, 35, 49, 56, 63, and 70.

Quantification and detection of sLrig1. To quantify the relative secretion of sLrig1 protein from multilayer capsules we carefully sorted 50 multilayer capsules using a dissection microscope (Leica MZ75 microsystems) The 50 individually sorted capsules were placed in 96 well plates and cultured in 100 μl of growth media. Culture supernatants were collected twice a week between day 14 - day 70 by replacing with fresh 100 μl of growth media. Quantification and detection of secreted sLrig1 was done by western blot using goat anti flag monoclonal antibody. Culture supernatant from encapsulated BHK control cells was used as negative control, whereas conditioned media from monolayer BHK-sLrig1 was used as positive control. From day 14 onwards, the volume of the cell culture media was doubled (100 μl to 200 μl) because of increase in cell growth in the capsules. Therefore the volume loaded on the gels was also doubled (to compensate for the 2x dilution). Briefly, 4 μl of culture supernatant of day 14 and 8 μl of culture supernatant from day 21 to day 70 from encapsulated cells were mixed in 1:1 ratio with 1x loading buffer (Invitrogen, Belgium) and resolved on 4–12% NuPAGE® Novex 4–12% Bis-Tris Gel (Invitrogen, Belgium) and transferred to polyvinylidene fluoride (PVDF) membranes (Invitrolon, Invitrogen, Belgium). ECL Advance™ blocking agent 2% (w/v) (GE Healthcare, UK) in Tris-buffered saline containing 0.1% Triton X-100 (TBST) was used for blocking PVDF membrane for at least 2 hours. Goat anti-FLAG mouse monoclonal antibody (1:50000) (Sigma, F1804) was used as primary antibody for the detection of recombinant FLAG-tagged sLrig1. Primary antibody was incubated overnight at 4°C. HRP-conjugated goat anti-mouse antibody (Jackson ImmunoResearch, 115-036-003) was used as secondary antibody (1:150000). The signal was visualized using an ECL™ Advance Western blot detection kit (GE Healthcare, UK). Bovine serum albumin (BSA) was used as housekeeping protein to confirm sample equal loading". BSA is visualized by nonspecific binding of secondary antibody. ECL image acquisition was performed with an ImageQuant LAS4010 imaging station and signals were quantified with Image Quant TL software (GE Healthcare, Belgium). Data was expressed as a relative percentage of the secretion at day 14.

Surface roughness of capsules. Surface roughness of different area of microcapsules was determined by atomic force microscopy (AFM). APA capsules without cells were used as control. Surface roughness of empty APA capsules (n=4), APA capsules (n=4) and multilayer capsules (n=4) with cells was studied on day 30 post-encapsulation using a Bruker dimensions 3100 atomic force microscopy. Topographic imaging of capsules was performed at room temperature using the tapping mode[21,60]. Briefly single capsules were carefully sorted using a dissection microscope (Leica MZ75 microsystems), washed with demineralized water and placed on microscopic slides. The excess of water was carefully aspirated. The surface of the microcapsules was scanned by the tip of a silicon nitride cantilever (Nanoprobes GmbH, Darmstadt, Germany), spring constant k was set to 0.05 N/m, which was vertically oscillating (z-oscillating) near its resonant frequency with a tapping frequency (x-y raster scanning) less than 1 Hz. Surface roughness (Rq) was evaluated by using the root mean square average of height deviations taken from the mean image data plane at a 5 μm scan. NanoScope V software was used to analyze the raw data of AFM.

Statistical analysis. Results are expressed as mean ± standard deviation (SD). Anova and Tukey tests were carried out using R software package, version 3.0.0. A p value <0.05 was considered statistically significant.

1. De Vos, P., Faas, M. M., Strand, B. & Calafiore, R. Alginate-based microcapsules for immunoisolation of pancreatic islets. *Biomaterials* **27**, 5603–5617 (2006).
2. Kulseng, B., Thu, B., Espevik, T., Skjak-Braek, G. & Skjåk-Braek, G. Alginate polylysine microcapsules as immune barrier: permeability of cytokines and immunoglobulins over the capsule membrane. *Cell Transplant.* **6**, 387–394 (1997).
3. Jacobs-Tulleneers-Thevissen, D. *et al.* Sustained function of alginate-encapsulated human islet cell implants in the peritoneal cavity of mice leading to a pilot study in a type 1 diabetic patient. *Diabetologia* **56**, 1605–14 (2013).
4. Jo K. Utvik & Simone, P. Niclou. in *Bioartifical Pancreas other Biohybrid Ther.* (Hallé, J.-P., Vos, P. De & Rosenberg, L.) 607–613 (Transworld Research Network, 2009).
5. Garcia, P. *et al.* Ciliary neurotrophic factor cell-based delivery prevents synaptic impairment and improves memory in mouse models of Alzheimer's disease. *J. Neurosci.* **30**, 7516–7527 (2010).
6. Emerich, D. F. & Salzberg, H. C. Update on immunoisolation cell therapy for CNS diseases. *Cell Transplant.* **10**, 3–24 (2001).
7. Emerich, D. F. *et al.* Protective effect of encapsulated cells producing neurotrophic factor CNTF in a monkey model of Huntington's disease. *Nature* **386**, 395–399 (1997).
8. Read, T. A. *et al.* Local endostatin treatment of gliomas administered by microencapsulated producer cells. *Nat. Biotechnol.* **19**, 29–34 (2001).
9. Johansson, M. *et al.* The soluble form of the tumor suppressor Lrig1 potently inhibits in vivo glioma growth irrespective of EGF receptor status. *Neuro. Oncol.* **15**, 1200–11 (2013).
10. Lohr, M. *et al.* Microencapsulated cell-mediated treatment of inoperable pancreatic carcinoma. *Lancet* **357**, 1591–1592 (2001).
11. Zimmermann, U. C., Jork, H., Thürmer, A., Zimmermann, F., Fuhr, H., Hasse, G. & Rothmund, C. M. in *Biotechnol. Spec. Process.* (H.J. Rehm, G. R.) 547–571 (Wiley-VCH Verlag GmbH, 2008).
12. Prüsse, U. *et al.* Comparison of different technologies for alginate beads production. *Chem. Pap.* **62**, 364–374 (2008).
13. Bhujbal, S. V., de Vos, P. & Niclou, S. P. Drug and Cell Encapsulation: Alternative Delivery Options for the Treatment of Malignant Brain Tumors. *Adv. Drug Deliv. Rev.* **67–68**, 142–53 (2014).
14. Terzis, A. J. A., Niclou, S. P., Rajcevic, U., Danzeisen, C. & Bjerkvig, R. Cell therapies for glioblastoma. *Expert Opin. Biol. Ther.* **6**, 739–49 (2006).
15. De Haan, B. J., Faas, M. M. & de Vos, P. Factors influencing insulin secretion from encapsulated islets. *Cell Transplant.* **12**, 617–25 (2003).
16. Uludag, H., De Vos, P. & Tresco, P. A. Technology of mammalian cell encapsulation. *Adv. Drug Deliv. Rev.* **42**, 29–64 (2000).
17. De Vos, P., Lazarjani, H. A., Poncelet, D. & Faas, M. M. Polymers in cell encapsulation from an enveloped cell perspective. *Adv. Drug Deliv. Rev.* (2013).
18. Stabler, C., Wilks, K., Sambanis, A. & Constantinidis, I. The effects of alginate composition on encapsulated betaTC3 cells. *Biomaterials* **22**, 1301–10 (2001).
19. Bhujbal, S. V., Paredes-Juarez, G. A., Niclou, S. P. & de Vos, P. Factors influencing the mechanical stability of alginate beads applicable for immunoisolation of mammalian cells. *J. Mech. Behav. Biomed. Mater.* **37C**, 196–208 (2014).
20. Joki, T. *et al.* Continuous release of endostatin from microencapsulated engineered cells for tumor therapy. *Nat. Biotechnol.* **19**, 35–9 (2001).
21. Bunger, C. M. *et al.* Biocompatibility and surface structure of chemically modified immunoisolating alginate-PLL capsules. *J. Biomed. Mater. Res. A* **67**, 1219–1227 (2003).
22. Orr, A. W., Helmke, B. P., Blackman, B. R. & Schwartz, M. A. Mechanisms of mechanotransduction. *Dev. Cell* **10**, 11–20 (2006).
23. García, J. R. & García, A. J. Cellular mechanotransduction: Sensing rigidity. *Nat. Mater.* **13**, 539–40 (2014).
24. Huselstein, C. *et al.* Influence of mechanical stress on cell viability. *Biorheology* **43**, 371–5 (2006).
25. Constantinidis, I., Rask, I., Long, R. C. & Sambanis, A. Effects of alginate composition on the metabolic, secretory, and growth characteristics of entrapped beta TC3 mouse insulinoma cells. *Biomaterials* **20**, 2019–27 (1999).
26. Haug, A. & Smidsrød, O. Selectivity of Some Anionic Polymers for Divalent Metal Ions. *Acta Chem. Scand* **3**, 843–854 (1970).
27. Mørch, Y. A., Donati, I., Strand, B. L. & Skjak-Braek, G. Effect of Ca2+, Ba2+, and Sr2+ on alginate microbeads. *Biomacromolecules* **7**, 1471–1480 (2006).
28. Chan, E.-S. *et al.* Effect of formulation of alginate beads on their mechanical behavior and stiffness. *Particuology* **9**, 228–234 (2011).
29. Goldmann, W. H. Mechanotransduction in cells. *Cell Biol. Int.* **36**, 567–70 (2012).
30. Ross, T. D. *et al.* Integrins in mechanotransduction. *Curr. Opin. Cell Biol.* **25**, 613–8 (2013).
31. Puklin-Faucher, E. & Sheetz, M. P. The mechanical integrin cycle. *J. Cell Sci.* **122**, 179–86 (2009).
32. Matthews, B. D., Overby, D. R., Mannix, R. & Ingber, D. E. Cellular adaptation to mechanical stress: role of integrins, Rho, cytoskeletal tension and mechanosensitive ion channels. *J. Cell Sci.* **119**, 508–18 (2006).

33. Huang, X. *et al.* Matrix stiffness in three-dimensional systems effects on the behavior of C3A cells. *Artif. Organs* **37**, 166–74 (2013).

34. Tam, S. K. *et al.* Biocompatibility and physicochemical characteristics of alginate-polycation microcapsules. *Acta Biomater.* **7**, 1683–92 (2011).

35. Vos, P. De. *et al* Effect of the alginate composition on the biocompatibility of alginate-polylysine microcapsules. *Biomaterials* **18**, 273–278 (1997).

36. Orive, G., Tam, S. K., Pedraz, J. L. J. L., Hallé, J.-P. & Hallé, J.-P. Biocompatibility of alginate-poly-L-lysine microcapsules for cell therapy. *Biomaterials* **27**, 3691–700 (2006).

37. Tam, S. K. *et al.* Factors influencing alginate gel biocompatibility. *J. Biomed. Mater. Res. A* **98**, 40–52 (2011).

38. De Vos, P. *et al.* Multiscale requirements for bioencapsulation in medicine and biotechnology. *Biomaterials* **30**, 2559–70 (2009).

39. De Vos, P., de Haan, B. J., Kamps, J. A. A. M., Faas, M. M. & Kitano, T. Zeta-potentials of alginate-PLL capsules: a predictive measure for biocompatibility? *J. Biomed. Mater. Res. A* **80**, 813–9 (2007).

40. De Vos, P., Hoogmoed, C. G. & Busscher, H. J. Chemistry and biocompatibility of alginate-PLL capsules for immunoprotection of mammalian cells. *J. Biomed. Mater. Res.* **60**, 252–9 (2002).

41. De Vos, P., van Hoogmoed, C. G., de Haan, B. J. & Busscher, H. J. Tissue responses against immunoisolating alginate-PLL capsules in the immediate posttransplant period. *J. Biomed. Mater. Res.* **62**, 430–437 (2002).

42. Strand, B. L. *et al.* Alginate-polylysine-alginate microcapsules: effect of size reduction on capsule properties. *J. Microencapsul.* **19**, 615–630 (2002).

43. Strand, B. L. *et al.* Poly-L-Lysine induces fibrosis on alginate microcapsules via the induction of cytokines. *Cell Transplant.* **10**, 263–275 (2001).

44. Juste, S., Lessard, M., Henley, N., Ménard, M. & Hallé, J.-P. Effect of poly-L-lysine coating on macrophage activation by alginate-based microcapsules: assessment using a new in vitro method. *J. Biomed. Mater. Res. A* **72**, 389–98 (2005).

45. Vandenbossche, G. M. *et al.* Host reaction against empty alginate-polylysine microcapsules. Influence of preparation procedure. *J. Pharm. Pharmacol.* **45**, 115–120 (1993).

46. Zhao, W. *et al.* Oxygen diffusivity in alginate/chitosan microcapsules. *J. Chem. Technol. Biotechnol.* **88**, 449–455 (2013).

47. Kuijlen, J. M. *et al.* The efficacy of alginate encapsulated CHO-K1 single chain-TRAIL producer cells in the treatment of brain tumors. *J. Neurooncol.* **78**, 31–39 (2006).

48. De Vos, P., Spasojevic, M., de Haan, B. J. & Faas, M. M. The association between in vivo physicochemical changes and inflammatory responses against alginate based microcapsules. *Biomaterials* **33**, 5552–9 (2012).

49. Thu, B. *et al.* Inhomogeneous alginate gel spheres: an assessment of the polymer gradients by synchrotron radiation-induced X-ray emission, magnetic resonance microimaging, and mathematical modeling. *Biopolymers* **53**, 60–71 (2000).

50. Thu, B., Skjåk-Bræk, G., Micali, F., Vittur, F. & Rizzo, R. The spatial distribution of calcium in alginate gel beads analysed by synchrotron-radiation induced X-ray emission (SRIXE). *Carbohydr. Res.* **297**, 101–105 (1997).

51. Machida-Sano, I. *et al.* Surface characteristics determining the cell compatibility of ionically cross-linked alginate gels. *Biomed. Mater.* **9**, 025007 (2014).

52. Lekka, M., Sainz-Serp, D., Kulik, A. J. & Wandrey, C. Hydrogel microspheres: influence of chemical composition on surface morphology, local elastic properties, and bulk mechanical characteristics. *Langmuir* **20**, 9968–77 (2004).

53. De Vos, P., De Haan, B., Pater, J. & Van Schilfgaarde, R. Association between capsule diameter, adequacy of encapsulation, and survival of microencapsulated rat islet allografts. *Transplantation* **62**, 893–899 (1996).

54. De Vos, P., De Haan, B. J., Wolters, G. H., Strubbe, J. H. & Van Schilfgaarde, R. Improved biocompatibility but limited graft survival after purification of alginate for microencapsulation of pancreatic islets. *Diabetologia* **40**, 262–270 (1997).

55. Zimmermann, H. *et al.* Physical and biological properties of barium cross-linked alginate membranes. *Biomaterials* **28**, 1327–45 (2007).

56. Albrecht, K., Christian, S., Jörg, B., Birgit, K. & Jörg, K. in *Acoust. Imaging* (Maev, R. G.) 223–229 (Plenum Publishers, New York, 2002). doi:10.1007/978-1-4419-8606-1_29.

57. Wang, C. X., Cowen, C., Zhang, Z. & Thomas, C. R. High-speed compression of single alginate microspheres. *Chem. Eng. Sci.* **60**, 6649–6657 (2005).

58. De Vos, P., De Haan, B. J. & Van Schilfgaarde, R. Upscaling the production of microencapsulated pancreatic islets. *Biomaterials* **18**, 1085–90 (1997).

59. Van Schilfgaarde, R. & de Vos, P. Factors influencing the properties and performance of microcapsules for immunoprotection of pancreatic islets. *J. Mol. Med. (Berl).* **77**, 199–205 (1999).

60. Siedlecki, C. A. & Marchant, R. E. Atomic force microscopy for characterization of the biomaterial interface. *Biomaterials* **19**, 441–54 (1998).

Author contributions

Additional information